

Supporting Information:

Nitrogen/Carbon Atomic Ratio-Dependent Performances of Nitrogen-Doped Carbon-Coated Metal Oxide Nanocrystals for Anodes in Lithium-Ion Batteries

Yemeng Ni,^a Yajing Yin,^{a,b} Ping Wu,^{a*} Hui Zhang,^a Chenxin Cai^{a*}

^a *Jiangsu Key Laboratory of New Power Batteries, Jiangsu Collaborative Innovation Center of Biomedical Functional Materials, College of Chemistry and Materials Science, Nanjing Normal University, Nanjing 210097, P. R. China.*

^b *Jiangsu Second Normal University, Nanjing 210013, P. R. China.*

* Corresponding author, E-mail: wuping@njnu.edu.cn, cxcai@njnu.edu.cn (C. Cai)

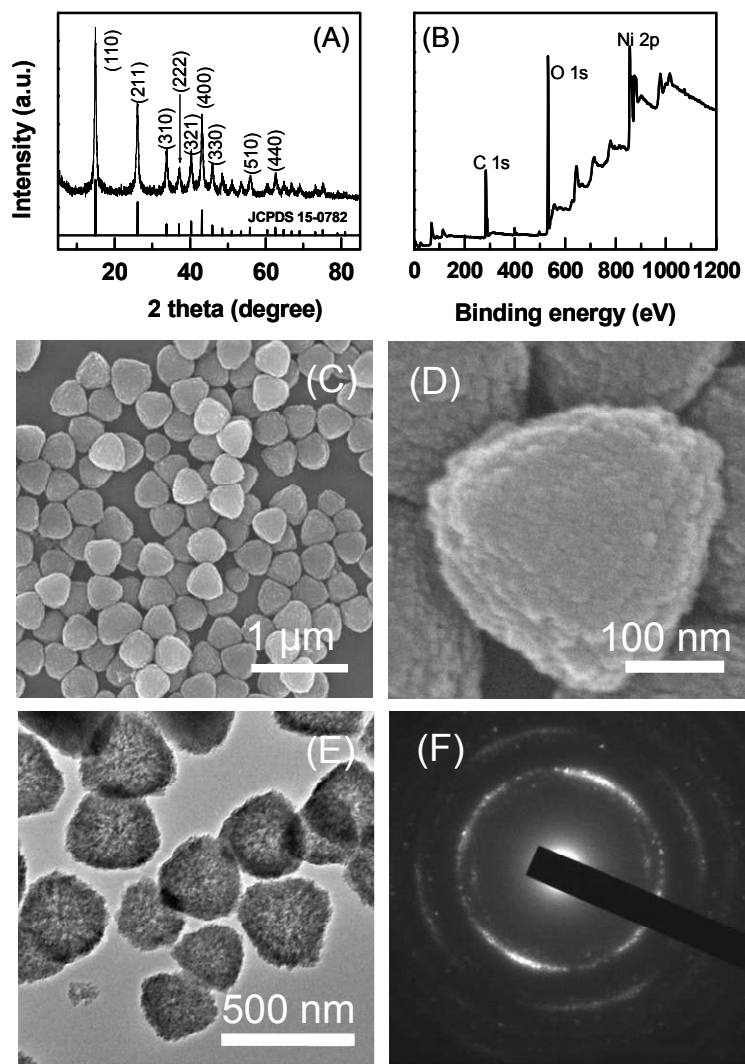


Figure S1. XRD patterns (A), XPS (B), SEM (C, D), and TEM images (E) of the as-prepared $\text{Ni}(\text{HCO}_3)_2$ precursors. (F) Typical SAED patterns of the prepared $\text{Ni}(\text{HCO}_3)_2$ precursors.

XRD patterns confirm the formation of $\text{Ni}(\text{HCO}_3)_2$ precursor because all the peaks observed can be indexed to characteristic peaks ((110), (211), (310), (222), (321), (400), (330), (510), and (440)) of $\text{Ni}(\text{HCO}_3)_2$ with body-centered cubic structure (JCPDS No. 15-0782) (Figure S1A). No peaks corresponding to other substances such as $\text{Ni}(\text{OH})_2$ or $\text{Ni}_2(\text{OH})_2\text{CO}_3$ are observed. XPS indicates the presence of Ni (855.9 eV), C (284.6 eV), and O (531.6 eV) elements in the precursor with the Ni, C, O atomic ratio of $\sim 1:2.2:6.3$ (evaluated by integrating the area under the correspondent peaks) (Figure S1B), which is in accordance with the theoretical one. These results demonstrate that we have prepared the $\text{Ni}(\text{HCO}_3)_2$ precursor. SEM (Figure S1C, D) and TEM images (Figure S1E) show the precursor has a

triangle-like shape with the size of ~280–320 nm and are composed by numerous small particles with the size of about 10–20 nm (Figure S1D). The selected area electron diffraction (SAED) pattern (Figure S1F) of the synthesized precursor shows concentric rings composed of bright discrete diffraction spots, indicating that the prepared $\text{Ni}(\text{HCO}_3)_2$ is polycrystalline with a high degree of crystallinity.

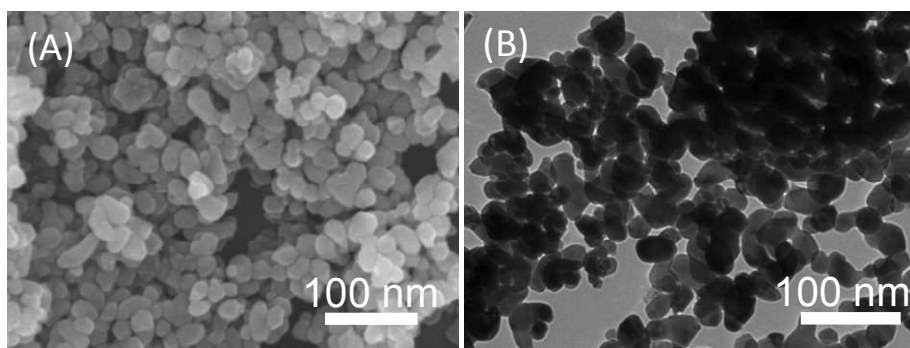


Figure S2. The SEM (A) and TEM images (B) of the prepared pristine NiO NPs.

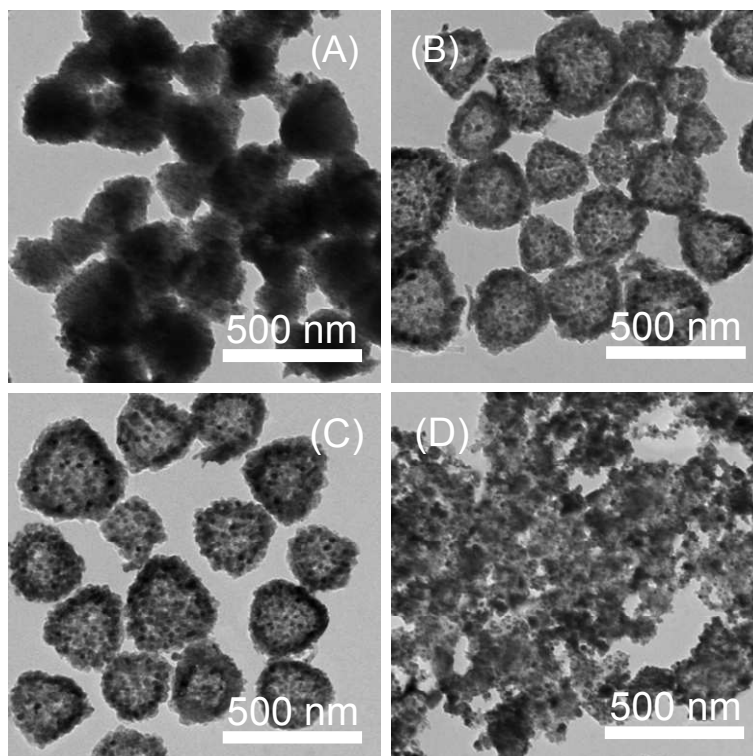


Figure S3. Dependence of the morphologies of the EM-N-C-NiO NCs on the time of the heat treatment of the $\text{Ni}(\text{HCO}_3)_2$ precursors in EMImBF₄. The heat treatment time is: (A) 2, (B) 3, (C) 4, and (D) 5 h.

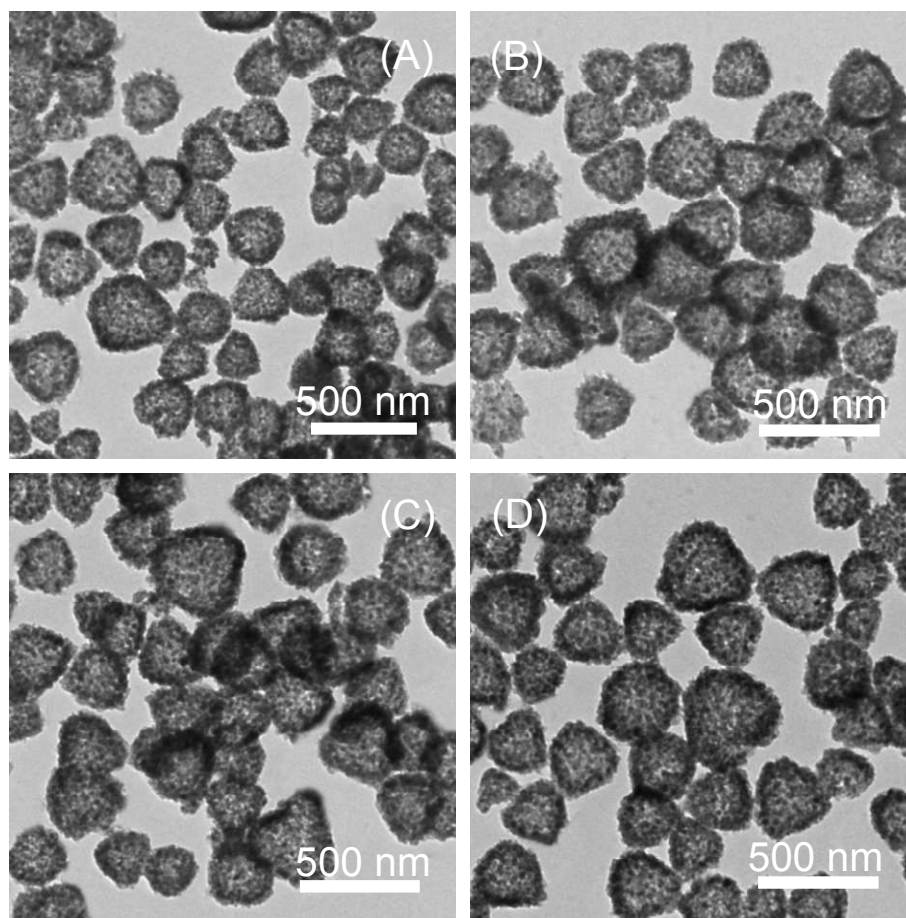


Figure S4. Dependence of the morphologies of the prepared EM-N-C-NiO NCs on the heat treatment temperature of the $\text{Ni}(\text{HCO}_3)_2$ precursors in EMImBF_4 . The heat treatment temperature is: (A) 120, (B) 150, (C) 180, and (D) 210 °C. The heat treatment time is 4 h.

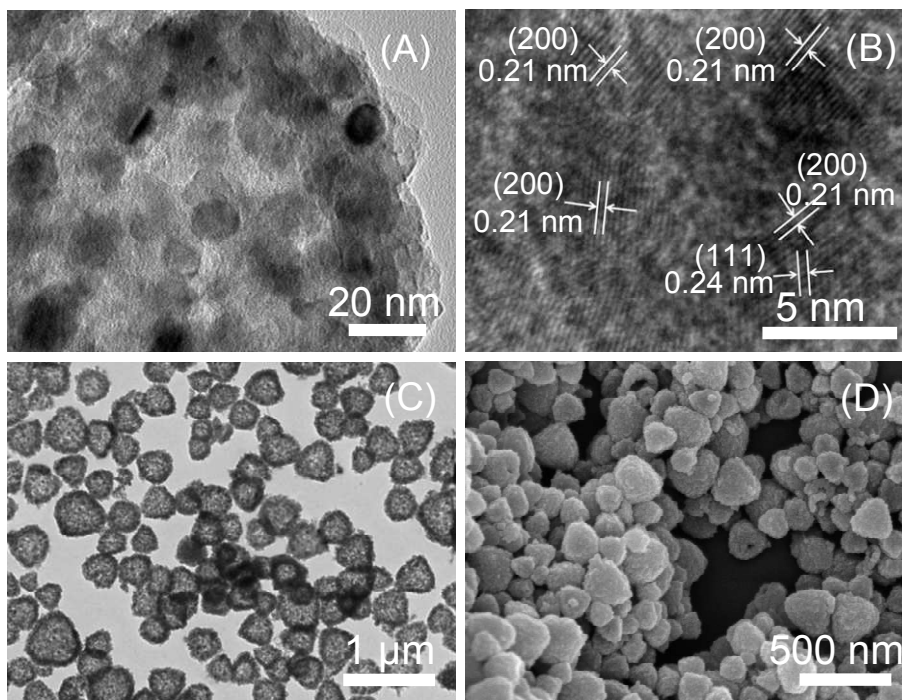


Figure S5. TEM (A, C), HRTEM (B), and SEM images (D) of the prepared BM-N-C-NiO NCs. The N-C-NiO NCs are assembled to form hollow structured cluster networks with sizes of ~250–300 nm. The BM-N-C-NiO NCs were obtained by calcining the BMImBF₄-coated Ni(HCO₃)₂ for 3 h at 350 °C under Ar atmosphere. The BMImBF₄-coated Ni(HCO₃)₂ were prepared by heat treatment of the Ni(HCO₃)₂ precursors in EMImBF₄ for 3–4 h at 180 °C.

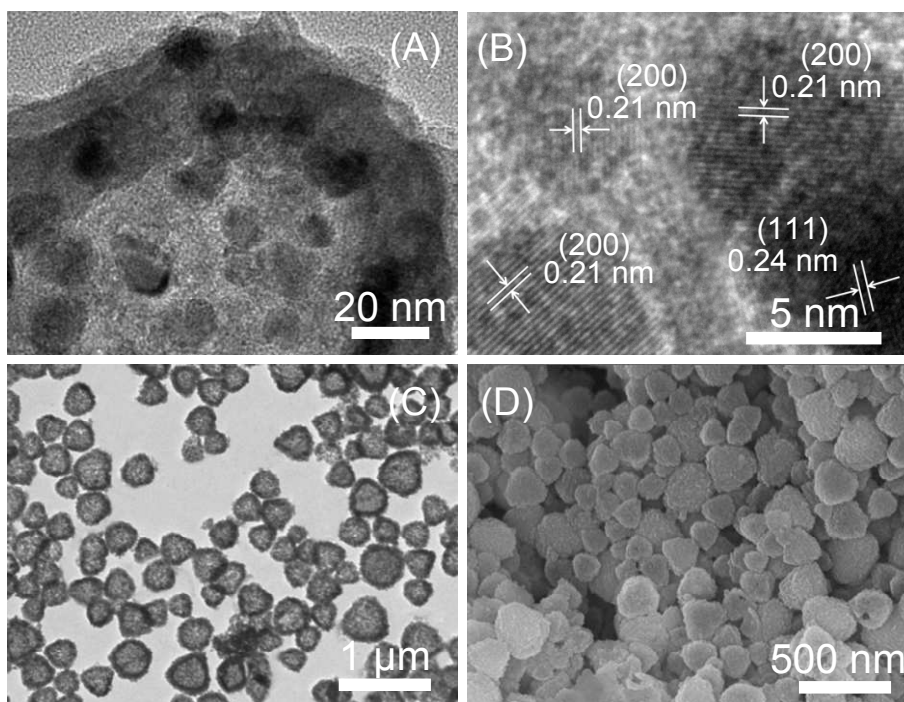


Figure S6. TEM (A, C), HRTEM (B), and SEM images (D) of the prepared HM-N-C-NiO NCs. The N-C-NiO NCs are assembled to form hollow structured cluster networks with sizes of ~250–300 nm. The HM-N-C-NiO NCs were obtained by calcining the HMI_mBF₄-coated Ni(HCO₃)₂ for 3 h at 350 °C under Ar atmosphere. The HMI_mBF₄-coated Ni(HCO₃)₂ were prepared by heat treatment of the Ni(HCO₃)₂ precursors in EMImBF₄ for 3–4 h at 180 °C.

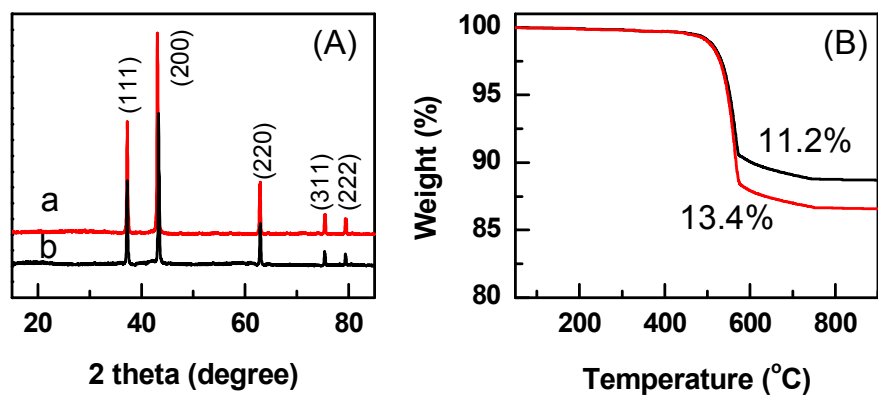


Figure S7. XRD patterns (A) and TGA measurements (B) of the BM-N-C-NiO NCs (curve a) and HM-N-C-NiO NCs (curve b).

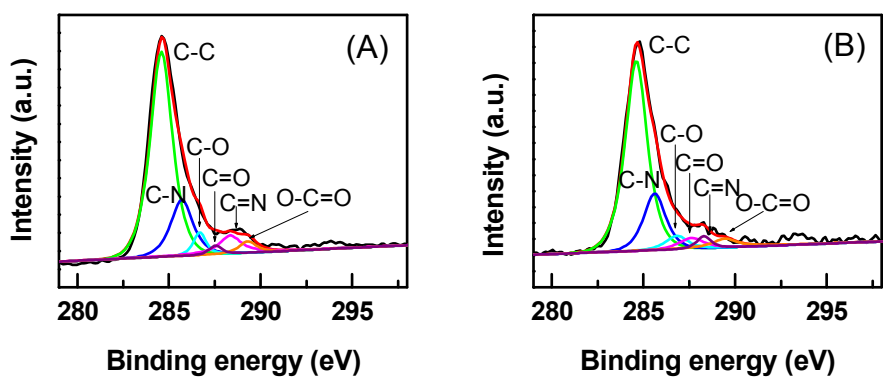


Figure S8. High resolution XPS spectra of C1s and their related curve-fitted components for the BM-N-C-NiO NCs (A) and HM-N-C-NiO NCs (B).

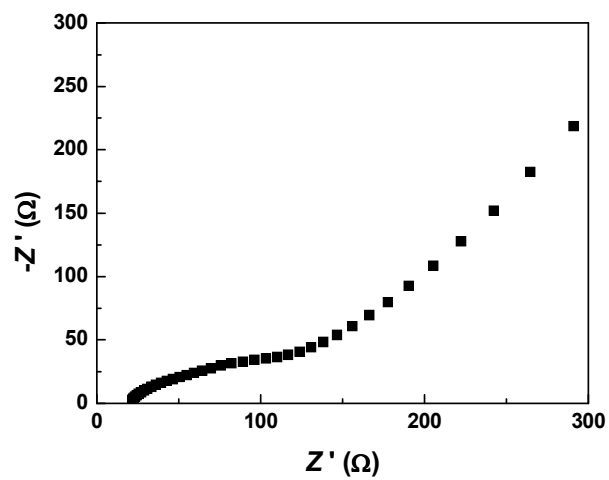


Figure S9. Electrochemical impedance spectra of the fresh pristine NiO NPs electrode in a coin half cell over the frequency range from 100 kHz to 0.01 Hz.